

See discussions, stats, and author profiles for this publication at: <https://www.researchgate.net/publication/281056018>

Production of Hydroxyl Radical via the Activation of Hydrogen Peroxide by Hydroxylamine

ARTICLE *in* ENVIRONMENTAL SCIENCE & TECHNOLOGY · AUGUST 2015

Impact Factor: 5.33 · DOI: 10.1021/acs.est.5b00483 · Source: PubMed

READS

290

7 AUTHORS, INCLUDING:



Liwei Chen

Nanjing Forestry University

8 PUBLICATIONS 209 CITATIONS

SEE PROFILE



Xuchun Li

Zhejiang Gongshang University

21 PUBLICATIONS 367 CITATIONS

SEE PROFILE



Jingyun Fang

Sun Yat-Sen University

23 PUBLICATIONS 423 CITATIONS

SEE PROFILE



Jun Ma

Harbin Institute of Technology

319 PUBLICATIONS 4,942 CITATIONS

SEE PROFILE

Production of Hydroxyl Radical via the Activation of Hydrogen Peroxide by Hydroxylamine

Liwei Chen,^{*,†} Xuchun Li,[§] Jing Zhang,^{||} Jingyun Fang,[⊥] Yanmin Huang,[†] Ping Wang,[†] and Jun Ma^{*,‡}

[†]College of Biology and the Environment, Nanjing Forestry University, Nanjing 210037, China

[§]School of Environmental Science and Engineering, Zhejiang Gongshang University, Hangzhou 310018, China

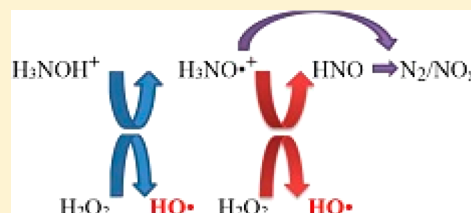
^{||}College of Architecture and Environment, Sichuan University, Chengdu 610065, China

[⊥]School of Environmental Science and Engineering, Sun Yat-sen University, Guangzhou 510275, China

[‡]State Key Laboratory of Urban Water Resource and Environment, Harbin Institute of Technology, Harbin 150090, China

Supporting Information

ABSTRACT: The production of the hydroxyl radical ($\text{HO}\cdot$) is important in environmental chemistry. This study reports a new source of $\text{HO}\cdot$ generated solely from hydrogen peroxide (H_2O_2) activated by hydroxylamine (HA). Electron paramagnetic resonance analysis and the oxidation of a $\text{HO}\cdot$ probe, benzoic acid, were used to confirm the production of $\text{HO}\cdot$. The production of $\text{HO}\cdot$ increased with increasing concentrations of either HA or H_2O_2 as well as decreasing pH. The second-order rate constant for the reaction was $(2.2 \pm 0.2) \times 10^{-4} \text{ M}^{-1} \text{ s}^{-1}$. $\text{HO}\cdot$ was probably produced in two steps: the activation of H_2O_2 by protonated HA and then reaction between the H_2O_2 and the intermediate protonated aminoxyl radical generated in the first step. Such a two-step oxidation can possibly be ascribed to the ionizable hydroxyl moiety in the molecular structure of HA, as is suggested by comparing the reactivity of a series of HA derivatives in $\text{HO}\cdot$ production. The results shed light on a previously unknown source of $\text{HO}\cdot$ formation, which broadens the understanding of its role in environmental processes.



INTRODUCTION

The hydroxyl radical ($\text{HO}\cdot$) is a most reactive species which can oxidize most organic substrates unselectively.^{1,2} It has been widely employed to degrade an enormous variety of recalcitrant and toxic contaminants in advanced oxidation processes (AOPs) such as the Fenton reaction, radiolysis, UV/ H_2O_2 purification, O_3 oxidation, and electrochemistry.^{3,4} The mechanisms of $\text{HO}\cdot$ generation and the involvement of $\text{HO}\cdot$ in redox reactions with contaminants in the environment have been investigated intensely for decades.^{2–5} $\text{HO}\cdot$ is usually produced via metal-involved reactions such as the Fenton reaction or using energy-input systems as in H_2O_2 /UV purification.^{6,7} However, metal-independent and energy-input free production of $\text{HO}\cdot$ has been reported occasionally,^{8–12} an intriguing and attractive finding.

The mechanism of metal-independent production of $\text{HO}\cdot$ is still under discussion, but it has been established that halogenated quinones and some reducing organic species such as ascorbic acid, phenols, hydroquinone and semiquinone moieties in reduced humic acid and biochar can enable the generation of active radicals with oxidants.^{8–12} One of the underlying mechanisms involves nucleophilic attack of halogenated quinones by H_2O_2 ; their product then decomposes homolytically to produce $\text{HO}\cdot$.⁸ Another mechanism involves electron transfer. Ascorbic acid undergoes a two-step oxidation by H_2O_2 to yield $\text{HO}\cdot$ and dehydroascorbic acid with the formation of an intermediate ascorbyl radical,⁹ and hydroquinone moieties in reduced humic acids are known to reduce

O_2 to form H_2O_2 and semiquinones, which then react with the H_2O_2 to generate $\text{HO}\cdot$.¹⁰ Semiquinone-type persistent free radicals in biochar can react directly with H_2O_2 by single-electron transfer and reduce it to $\text{HO}\cdot$.¹¹ Moreover, phenols can activate persulfate to form sulfate radicals, which are then transformed to $\text{HO}\cdot$ with hydroxide at alkaline pH or water at lower pH.¹² The common feature linking ascorbic acid, phenols, reduced humic acids, and biochar is the possession of ionizable hydroxyl moiety or a relevant C-centered radical which can participate in the production of $\text{HO}\cdot$.^{9–12}

Hydroxylamine (HA), a widely used reductant and antioxidant,¹³ contains an ionizable hydroxyl moiety and can undergo electron transfer or H atom abstraction.^{14–17} Previous work in our laboratory has indicated that it can accelerate Fe(II)/Fe(III) redox cycles to enhance the generation of reactive radicals dramatically in a Fenton system or an Fe(II)/peroxymonosulfate system.^{18,19} Considering its similar reducing activity and the ionizable hydroxyl group, it is hypothesized that HA may activate H_2O_2 to form $\text{HO}\cdot$ without a transition metal. Radical species are very probably produced as intermediates in the electron transfer process between H_2O_2 and HA,²⁰ though the mechanism of $\text{HO}\cdot$ production involving HA and H_2O_2 is still unknown.

Received: January 28, 2015

Revised: August 10, 2015

Accepted: August 14, 2015

The objectives of this study were to explore the potential of the reaction between HA and H_2O_2 as a new source of $\text{HO}\cdot$ and to reveal the mechanism involved. Electron paramagnetic resonance (EPR) technique and the oxidation of a $\text{HO}\cdot$ probe benzoic acid (BA) were used to illustrate the $\text{HO}\cdot$ production. The effects of pH and the concentrations of HA and H_2O_2 on $\text{HO}\cdot$ production were explored, and the potential pathways for $\text{HO}\cdot$ generation will be discussed. By studying $\text{HO}\cdot$ production by H_2O_2 with a series of HA derivatives (HAs), the role of ionizable hydroxyl moiety in the molecular structure of the HAs during the process was revealed and a plausible mechanism can now be proposed.

MATERIALS AND METHODS

Materials. All of the chemicals listed in Text S1 of the Supporting Information were used as purchased without further purification. Stock solutions of HA and its derivatives were all freshly prepared using deaerated Milli-Q water (deaerated using nitrogen).

Experimental Procedures. The EPR experiments were conducted at room temperature on a Bruker A200 300E instrument. Solutions of H_2O_2 , HA, the spin-trapping agent 5,5-dimethyl-1-pyrroline N-oxide (DMPO), transition metal ions, $\text{HO}\cdot$ scavengers or iron chelators were mixed and deaerated with nitrogen. They were buffered at the desired pH with perchloric acid or acetate for the detection of $\text{HO}\cdot$. The possible influence of perchloric acid on the system was negligible (Figure S1 and Text S2 in the Supporting Information). After mixing for about 1 min (± 3 s), the sample solution was transferred into a 100 μL capillary tube, which was then fixed in the cavity of the EPR spectrometer. Ethyl *N*-hydroxycarbamate (a derivative of HA) was similarly mixed with H_2O_2 for the detection of relevant aminoxyl radicals.²¹

All of the other experiments were carried out in triangular flasks with constant stirring using a PTFE-coated magnetic stirrer in Milli-Q water adjusted to pH 3.0 with perchloric acid and deaerated with nitrogen throughout the experiments. The concentration of dissolved oxygen (DO) in the solution was below the detection limit of a DO meter (less than 0.31 μM). The solutions' temperature was maintained at 25 ± 0.5 $^\circ\text{C}$. All of the experiments were performed at least in duplicate. In each run, HA, BA, perchloric acid, or *tert*-butanol were mixed in the desired dosages and the experiment was switched on by adding the desired dosage of H_2O_2 . The pH changed less than 0.1 unit during the experiments. To avoid the interference of nitrogen in the detection of N_2O generated in the system, argon (Ar, 99.99%) instead of nitrogen was used to remove oxygen in the solution before the initiation of the reaction. The flasks were totally sealed to prevent the escape of N_2O from the solution and to guarantee the oxygen-free conditions during the process.

Sample Analysis. The concentrations of BA, *m*-hydroxybenzoic acid (MHBA), *o*-hydroxybenzoic acid (OHBA), and *p*-hydroxybenzoic acid (PHBA) were determined on high performance liquid chromatography (HPLC, Dionex Ultimate 3000) equipped with a reverse-phase C18 column. The pH was measured with a Denver Instrument Ultrabasic 10 pH meter. The concentration of DO was measured by a DO meter (Rex Electric Chemical, JPSJ-605). The H_2O_2 concentrations were measured by a colorimetric method using peroxidase and *N,N*-diethyl-*p*-phenylenediamine (DPD) on a PE Lambda 25 UV-vis spectrometer.²² The HA samples were derivatized to acetone oxime using acetone and were subsequently extracted using methyl *tert*-butyl ether (MTBE). The acetone oxime

concentrations were measured using a Shimadzu GC-2010 gas chromatograph with a flame ionization detector (FID) and N_2 as the carrier gas.²³ Ion chromatography (Dionex ICS-900) was employed for the detection of NO_2^- and NO_3^- . The concentration of dissolved N_2O was analyzed using a gas chromatograph (Agilent 7890) equipped with an electron capture detector (ECD) and a headspace sampler.^{19,24} Additional details of the sample analysis procedures are presented in Text S3 of the Supporting Information.

RESULTS AND DISCUSSION

$\text{HO}\cdot$ Production. Figure 1a shows typical EPR signals of DMPO–OH during the reaction of HA with H_2O_2 . The typical

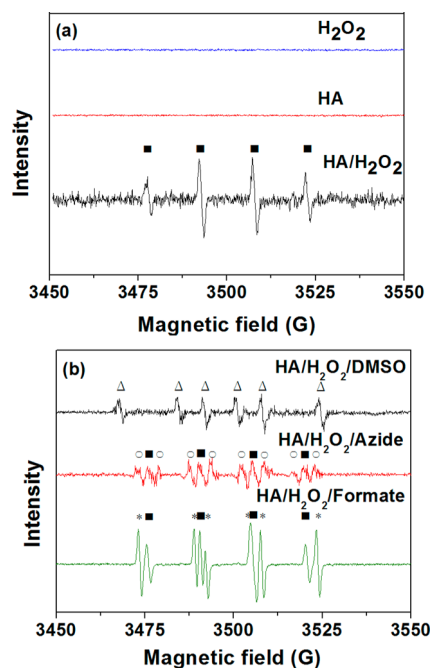
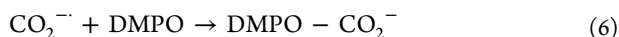
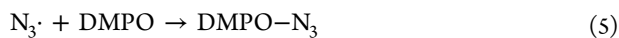
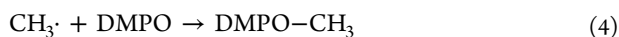
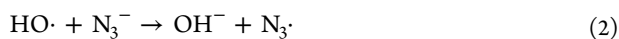
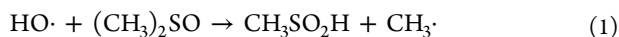


Figure 1. EPR signals of DMPO spin trapping adducts produced by (a) HA and H_2O_2 , and (b) HA and H_2O_2 in the presence of $\text{HO}\cdot$ scavengers. Reaction conditions: $[\text{DMPO}]_0 = 20.0$ mM, $[\text{H}_2\text{O}_2]_0 = 10.0$ mM, $[\text{HA}]_0 = 10.0$ mM, $[\text{scavengers}]_0 = 500.0$ mM, pH = 3.0, 25 $^\circ\text{C}$, DMPO–OH, ■; DMPO–CH₃, △; DMPO–N₃, ○; DMPO–CO₂[−], *.

DMPO–OH spin adduct ($a^{\text{H}} = a^{\text{N}} = 14.9$ G), which has a specific quartet spectrum with peak height ratios of 1:2:2:1, indicates the formation of $\text{HO}\cdot$.²⁵ It should be noted that a similar DMPO–OH signal may arise from the decomposition of DMPO–OOH and the nucleophilic addition to DMPO in the presence of Fe(III) or Cu(II).^{26,27} Additional analysis was therefore carried out to confirm the production of $\text{HO}\cdot$. Dimethyl sulfoxide (DMSO), azide, and formate react with $\text{HO}\cdot$ to generate methyl radicals ($\text{CH}_3\cdot$), azidyl radicals ($\text{N}_3\cdot$), and carbon dioxide anion radicals ($\text{CO}_2^{\cdot-}$), respectively, as shown in the equations (eqs 1–3). These intermediate radicals can also be captured by DMPO to yield the corresponding DMPO–CH₃ ($a^{\text{H}} = 23.4$ G, $a^{\text{N}} = 16.4$ G), DMPO–N₃ ($a^{\text{H}} = a^{\text{N}} = 14.7$ G), and DMPO–CO₂[−] ($a^{\text{H}} = 19.3$ G, $a^{\text{N}} = 15.9$ G) spin adducts (eqs 4–6).²⁶ DMSO, azide, and formate were therefore adopted in the EPR study to verify the formation of $\text{HO}\cdot$. The spin adducts of DMPO–CH₃, DMPO–N₃, and DMPO–CO₂[−] were generated instead of DMPO–OH when excessive DMSO, azide or formate was present in the system, accompanied by a

marked decrease in or disappearance of the DMPO–OH spin adducts (Figure 1b). These EPR results indicate the generation of HO· in the system.



Further evidence comes from the inhibition effect of *tert*-butyl alcohol (TBA), which is a strong HO· scavenger ($k_{\text{TBA, HO}\cdot} = 7.6 \times 10^8 \text{ M}^{-1} \text{ s}^{-1}$),²⁸ on the competition of HO· with BA, the HO· probe. Figure S2 shows almost complete inhibition of BA oxidation by 0.1 M TBA, suggesting the dominant contribution of HO· to BA oxidation in the system. Moreover, the *m*-hydroxybenzoic acid (MHBA), *o*-hydroxybenzoic acid (OHBA), and *p*-hydroxybenzoic acid (PHBA) are the primary intermediates, so their detection during the oxidation of BA also helps confirm the involvement of HO· in the system.^{29,30} As is shown in Figure S3, MHBA, OHBA, and PHBA were all detected, further supporting the generation of HO·.

Possible Influence of Trace Transition Metal Ions.

Trace transition metal impurities in the reagents may possibly have enhanced the generation of HO·. As can be seen from Figure S4, only iron could notably enhance the intensity of the HO· signal. This was readily excluded by using ferrozine and ferene as iron chelators.²⁶ Almost complete disappearance of the DMPO–OH signal in a traditional Fenton system when ferrozine or ferene is present, confirms their excellent iron complexing ability, as shown in Figure S5. In contrast, no significant decrease in the intensity of the HO· signal was observed in the HA–H₂O₂ reactions in the presence of sufficient ferrozine or ferene (Figure 2), indicating that trace iron was not responsible for the HO· production. The generation of HO· by the reaction of HA and H₂O₂ is indeed metal-independent.

Effect of pH. Figure 3 presents the profiles of DMPO–OH spin adducts at pH ranging from 2.0 to 6.0. The intensity of the

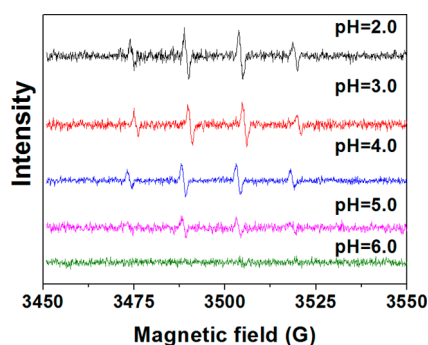


Figure 3. Effect of pH with acetate buffer on the EPR signals of DMPO–OH spin trapping adducts produced by HA and H₂O₂ in the pH range of 2.0 to 6.0. Reaction conditions: [DMPO]₀ = 20.0 mM, [H₂O₂]₀ = 10.0 mM, [HA]₀ = 10.0 mM, 25 °C.

HO· signal decreased with increasing pH, and it almost disappeared at pH values higher than 6.0.

The pK_a values for HA are 5.96 and 13.74.^{31,32} When the pH is less than 5, the majority of the HA is in its protonated form (H₃NOH⁺); it is mainly in its unprotonated form (H₂NOH) at pH values in the range of 7.0 to 12.0. The second-order rate constants for the reactions of HO· with H₃NOH⁺ and H₂NOH are $\leq 5.0 \times 10^8 \text{ M}^{-1} \text{ s}^{-1}$ and $9.5 \times 10^9 \text{ M}^{-1} \text{ s}^{-1}$, respectively,³³ so the scavenging of HO· by HA increases with increasing pH. In addition, some researchers have proposed that the protonated form of the hydroxylamino radical, the one-electron transfer intermediate of HA with a pK_a of about 4.2, reacts much faster with H₂O₂ than the unprotonated hydroxylamino radical to produce HO·.^{17,33} Under strongly acidic conditions, most of the hydroxylamino radical is protonated, and thus the HO· production increased with decreasing pH. The pH might therefore affect HO· generation mainly through controlling the species distribution of HA and the intermediate hydroxylamino radical.

Effect of HA and H₂O₂ Concentrations. The EPR results presented in Figure S6 show that the concentration of HO· increased with increasing concentrations of either HA or H₂O₂, indicating the involvement of the two reagents in the HO· generation. The reaction between H₂O₂ and H₃NOH⁺ was studied under acidic conditions by purging with N₂ constantly to minimize the influence of side reactions such as oxidation of unprotonated HA by HO·. Under those conditions the *k* was determined to be $(2.2 \pm 0.2) \times 10^{-4} \text{ M}^{-1} \text{ s}^{-1}$ (Text S4 and Figure S7 of the Supporting Information), which seems relatively low.

Role of the Molecular Structure of the Hydroxylamines. The contribution of the series of hydroxylamine derivatives (HAs, shown in Figure 4) to HO· generation with H₂O₂ was investigated. Figure 5 shows the individual DMPO–OH spin adduct in each HAs–H₂O₂ reaction. HO· production was observed in the case of *N*-methyl hydroxylamine (*N*-methyl HA), *N,N*-dimethyl hydroxylamine (*N,N*-dimethyl HA), *N-tert*-butyl hydroxylamine (*N-tert*-butyl HA), *N*-benzyl hydroxylamine (*N*-benzyl HA) and *N,O*-dimethyl hydroxylamine (*N,O*-dimethyl HA). *N*-methyl HA, *N,N*-dimethyl HA and *N-tert*-butyl HA were even more efficient than HA in producing HO·, but *N*-benzyl HA and *N,O*-dimethyl HA were much less reactive. And no HO· was detected under the same conditions with the *O*-Substituted HAs, for example, *O*-methyl HA, *O-tert*-butyl hydroxylamine (*O-tert*-butyl HA) and *O*-benzyl hydroxylamine (*O*-benzyl HA). *N*-Substituted HAs showed much

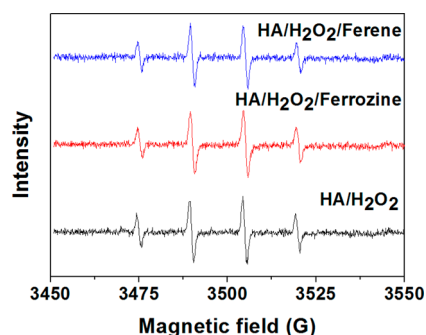


Figure 2. Effect of the iron chelating agents ferrozine and ferene on the EPR signals of DMPO–OH spin trapping adducts produced by HA and H₂O₂. Reaction conditions: [DMPO]₀ = 20.0 mM, [H₂O₂]₀ = 10.0 mM, [HA]₀ = 10.0 mM, [ferrozine]₀ = 50.0 μM, [ferene]₀ = 50.0 μM, pH = 3.0, 25 °C.

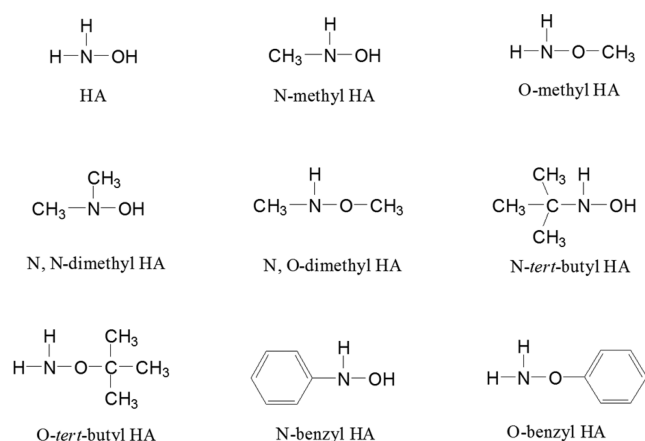


Figure 4. Chemical structures of the HAs used.

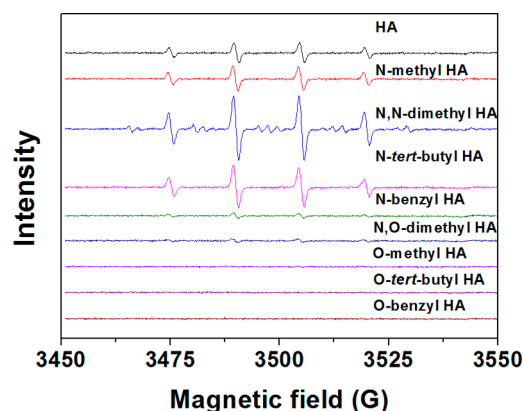


Figure 5. EPR signals of DMPO–OH spin trapping adducts produced by H_2O_2 and HAs. Reaction conditions: $[\text{DMPO}]_0 = 20.0 \text{ mM}$, $[\text{H}_2\text{O}_2]_0 = 10.0 \text{ mM}$, $[\text{HAs}]_0 = 10.0 \text{ mM}$, $\text{pH} = 3.0$, 25°C .

greater $\text{HO}\cdot$ generation than the O-Substituted HAs in the presence of H_2O_2 . This suggests that the production of $\text{HO}\cdot$ by H_2O_2 and HAs is probably related to the $-\text{OH}$ group in the structure of HAs.

Mechanism of $\text{HO}\cdot$ Generation. An intermediate aminoxyl radical ($\text{H}_2\text{NO}\cdot$) or its isomer hydroxylamino radical ($\cdot\text{HNOH}$) is formed during the oxidation of HA by a one-electron oxidant or an H atom abstractor.³⁴ Considering that the bond dissociation energy (BDE) of $\text{O}-\text{H}$ in HA (75 to 77 kcal M^{-1}) is weaker than that of $\text{N}-\text{H}$ (81 to 82 kcal M^{-1}),^{34,35} $\text{H}_2\text{NO}\cdot$ is more easily generated and stable than $\cdot\text{HNOH}$.³⁴ When $\text{HO}\cdot$ is generated by the reaction of HA and H_2O_2 through one electron transfer under acidic conditions, H_2O_2 presumably reacts with protonated HA to produce $\text{HO}\cdot$ and an aminoxyl radical via eq 7. To verify this hypothesis, ethyl *N*-hydroxycarbamate, an HA derivative, was reacted with H_2O_2 instead of HA to generate a more intense EPR signal of its corresponding aminoxyl radical.²¹ Despite its short lifetime,³⁵ the EPR signal shown in Figure 6 verified the generation of aminoxyl radical ($a^{\text{N}} = 7.2 \text{ G}$, $a^{\text{N}-\text{H}} = 11.4 \text{ G}$, $a^{\text{C}-\text{H}} = 0.9 \text{ G}$) in the system,²¹ supporting the pathway presented in eq 7.

The protonated form of the hydroxylamino radical ($\text{pK}_a \approx 4.2$) was reported to react with H_2O_2 much faster than the unprotonated hydroxylamino radical to produce $\text{HO}\cdot$ and nitroxyl (HNO).^{17,33} However, the aminoxyl radical has been proven to be the dominating active intermediate in one-electron oxidation of HA aforementioned.³⁴ Thus, we proposed

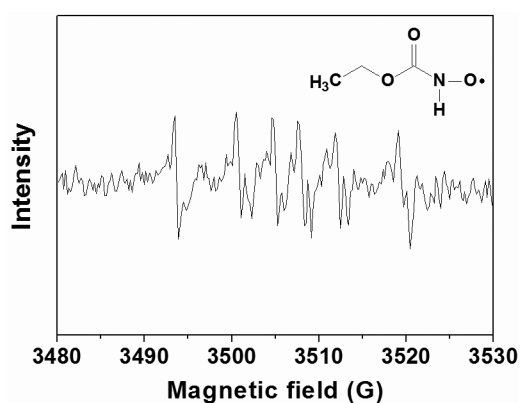
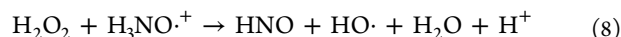
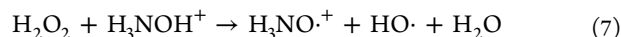
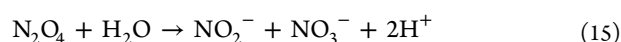
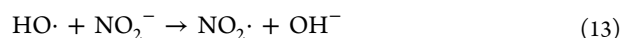
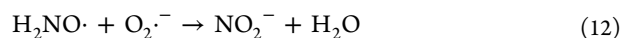
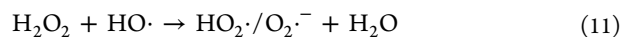


Figure 6. EPR signal of aminoxyl radical produced by H_2O_2 and ethyl *N*-hydroxycarbamate. Reaction conditions: $[\text{ethyl } N\text{-hydroxycarbamate}]_0 = 50.0 \text{ mM}$, $[\text{H}_2\text{O}_2]_0 = 50.0 \text{ mM}$, $\text{pH} = 3.0$, 25°C .

that the protonated form of the aminoxyl radical would react with H_2O_2 much faster to produce HNO and $\text{HO}\cdot$ via eq 8.



The aminoxyl radical and HNO , oxidation intermediates of HA, were ultimately converted to nitrogen and various nitrogen oxides (e.g., N_2O , NO_2^- , and NO_3^-) depending on the conditions.³⁴ The generation of gaseous products (N_2 and N_2O) mainly depends on the pH. The dimerization of unstable HNO to form N_2O is favored in strongly acidic conditions with the rate constant of $(4.5 \pm 2.7) \times 10^9 \text{ M}^{-1} \text{ s}^{-1}$ (eq 9).^{36–38} N_2 could be formed by the dimerization/cleavage of $\text{H}_2\text{NO}\cdot$ at pHs higher than 4.0 with a second-order rate constant of $(2.8 \pm 0.5) \times 10^8 \text{ M}^{-1} \text{ s}^{-1}$ (eq 10).^{17,20,34} In addition, reactions involving excess H_2O_2 might account for the production NO_3^- , and NO_2^- is probably formed as an intermediate (eqs 11–15).¹⁷ N_2O was (Figure S8 determined in the system at pH 3.0 to verify the formation of HNO indirectly, as HNO is unstable and it spontaneously dimerizes and subsequently dehydrates to form N_2O with a high rate constant.³⁸ Figure S8 in the Supporting Information also shows the concentration of NO_2^- and NO_3^- generated in the HA and H_2O_2 reaction. The generation of NO_2^- and NO_3^- was not so evident, and the gaseous products N_2O increased with longer reaction time, supporting the formation of HNO and the two-step oxidation pathway for $\text{HO}\cdot$ generation (eqs 7 and 8).



According to the former two-step oxidation hypothesis, the theoretical stoichiometric ratio of HA consumption to H_2O_2 depletion is 0.5 not only for protonated HA but also for the intermediate protonated aminoxyl radical reacting with H_2O_2

(eqs 7 and 8). To estimate the actual stoichiometric ratio in the system, BA was employed to scavenge HO·. The amount of HA consumed was then much lower than that of H₂O₂ (Figure 7a).

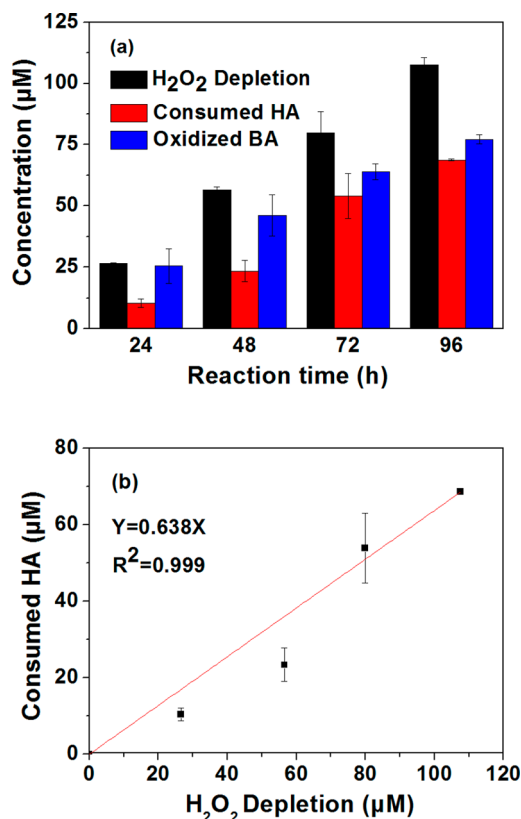


Figure 7. (a) The concentration changes of reagents and (b) the ratio of HA consumption to H₂O₂ depletion during the oxidation of BA by HA and H₂O₂. Reaction conditions: [BA]₀ = 0.4 mM, [H₂O₂]₀ = 0.4 mM, [HA]₀ = 0.4 mM, pH = 3.0, 25 °C.

The slope in Figure 7b shows that the stoichiometric ratio of HA consumption to H₂O₂ depletion was about 0.638, supporting the statement on the two major steps (eqs 7 and 8) involved in the reaction between HA and H₂O₂.

Figure 7a also shows the relationship between the oxidized BA and H₂O₂ depletion during the process. More than 95% of the depleted H₂O₂ was transformed to HO· to attack BA within 24 h. However, the ratio of oxidized BA to H₂O₂ depletion gradually decreased during the process. This may be because H₂O₂ competes with HO· to form NO₂[−] and NO₃[−] (eqs 11–15 and Figure S8),¹⁷ and some of the HO· that is consumed by the HA as the second-order rate constants of BA and HA with HO· are $4.3 \times 10^9 \text{ M}^{-1} \text{ s}^{-1}$ and $\leq 5.0 \times 10^8 \text{ M}^{-1} \text{ s}^{-1}$, respectively.^{1,34} Furthermore, the second-order kinetic constants for HO· attacking OHBA and PHBA are $2.7 \times 10^{10} \text{ M}^{-1} \text{ s}^{-1}$ and $8.0 \times 10^9 \text{ M}^{-1} \text{ s}^{-1}$, respectively,^{1,30} suggesting that HBAs are more reactive with HO· than BA. The total amounts of MHBA, OHBA, and PHBA only accounted for about half of the observed BA oxidation (Figure S3), so those primary products (OHBA, MHBA, and PHBA) formed in the system further compete with BA for HO· and yield other intermediate products as the reaction progresses.³⁹ Thus, the estimated concentration of HO· at $1.49 \times 10^{-16} \text{ M}$ based on the BA degradation kinetics (Figure S9) ought to be lower than the actual one in the system.

The two-step oxidation hypothesis is further demonstrated by the role of the molecular structure of the HAs (Figure 5). N-Substituted HAs with ionizable hydroxyl moiety showed much greater HO· generation than O-Substituted HAs. The BDE of the N–H bonds in HAs is 81 to 82 kcal M^{−1}, while the BDE of O–H bonds in the N-Substituted HAs illustrated here is less than 77 kcal M^{−1}.³⁵ Such N-Substituted HAs tend to yield aminoxyl radicals (R₂NO·) and HO· when reacting with H₂O₂, and the aminoxyl radicals may yield oxoammonium (RN=O) and HO· through reacting with H₂O₂ in acidic conditions. Furthermore, the substitution of –OH by methoxyl on the N atom weakens the N–H bond, leading to a low yield of R₂NO·.^{33–35} So N-Substituted HAs have much higher reactivity with H₂O₂ to produce HO· than O-Substituted ones. In addition, N,O-dimethyl HA shows insignificant reactivity to produce HO· because O-Substituted HAs can undergo only one-step oxidation with H₂O₂ to yield ·NROR and HO·. Consequently, it is hypothesized that the ionizable hydroxyl (–OH) moiety attached to an N atom of HAs is transformed to an =O moiety through the formation of an intermediate –O·. This may then be responsible for the production of HO· with H₂O₂.

Implication. This study has demonstrated a previously unrecognized pathway for the formation of HO· from HA and H₂O₂. These results highlight the significance of reactions between H₂O₂ and HA which might be catalyzed rapidly by some transition metals.^{14–16,38} It is therefore expected that HO· generation via eqs 7 and 8 will be greatly enhanced. Indeed, previous work in our laboratory has partially confirmed such a hypothesis in the case of Fenton reactions in the presence of HA.¹⁸ H₂O₂ and/or superoxide radicals (e.g., HO₂·) are ubiquitous in the aquatic environment,^{40,41} and the HA-like intermediates can be formed through the biodegradation of nitrogen-containing species (e.g., nitrogen fixation, nitrification, and denitrification).^{35,42} The findings of this study may therefore help to elucidate the redox dynamics of contaminants in natural processes.

■ ASSOCIATED CONTENT

Supporting Information

The Supporting Information is available free of charge on the ACS Publications website at DOI: 10.1021/acs.est.5b00483.

Four texts and nine figures are available with further information about the materials and additional data (PDF)

■ AUTHOR INFORMATION

Corresponding Authors

*(L.C.) Phone: +86-025-85427479; fax: +86-025-85418873; e-mail: chenliwei@njfu.edu.cn.

*(J.M.) Phone: +86-451-86282292; fax: +86-451-8628-3010; e-mail: majun@hit.edu.cn.

Notes

The authors declare no competing financial interest.

■ ACKNOWLEDGMENTS

This study was supported by the Natural Science Foundation of China (Grants 51408317, 21307057, and 51378515) and the Natural Science Foundation of Jiangsu Province (BK20140966 and BK20130577). Funds from the priority academic program development of Jiangsu higher education institutions (PAPD) are also gratefully acknowledged. The authors sincerely thank

Chengyue Sun, Associate Professor Jimin Shen, Jing Zou (Harbin Institute of Technology), Yunxia Sui (Nanjing University), Lei Yu, Qinhua Fan, and Qi Li (Nanjing Forestry University) for their technical help with the EPR, GC, and ion chromatography analysis.

REFERENCES

- (1) Buxton, G. V.; Greenstock, C. L.; Helman, W. P.; Ross, A. B. Critical review of rate constants for reactions of hydrated electrons, hydrogen atoms and hydroxyl radicals ($\cdot\text{OH}/\cdot\text{O}^-$) in aqueous solution. *J. Phys. Chem. Ref. Data* **1988**, *17*, 513–886.
- (2) Goldstone, J. V.; Pullin, M. J.; Bertilsson, S.; Voelker, B. M. Reactions of hydroxyl radical with humic substances: Bleaching, mineralization, and production of bioavailable carbon substrates. *Environ. Sci. Technol.* **2002**, *36* (3), 364–372.
- (3) Passananti, M.; Temussi, F.; Iesce, M. R.; Mailhot, G.; Brigante, M. The impact of the hydroxyl radical photochemical sources on the rivastigmine drug transformation in mimic and natural waters. *Water Res.* **2013**, *47* (14), 5422–5430.
- (4) Wang, J. L.; Xu, L. J. Advanced oxidation processes for wastewater treatment: Formation of hydroxyl radical and application. *Crit. Rev. Environ. Sci. Technol.* **2012**, *42* (3), 251–325.
- (5) White, E.; Vaughan, P.; Zepp, R. Role of the photo-Fenton reaction in the production of hydroxyl radicals and photobleaching of colored dissolved organic matter in a coastal river of the southeastern United States. *Aquat. Sci.* **2003**, *65* (4), 402–414.
- (6) Pignatello, J. J.; Oliveros, E.; MacKay, A. Advanced oxidation processes for organic contaminant destruction based on the Fenton reaction and related chemistry. *Crit. Rev. Environ. Sci. Technol.* **2006**, *36* (1), 1–84.
- (7) Chelme-Ayala, P.; El-Din, M. G.; Smith, D. W. Degradation of bromoxynil and trifluralin in natural water by direct photolysis and UV plus H_2O_2 advanced oxidation process. *Water Res.* **2010**, *44* (7), 2221–2228.
- (8) Zhu, B. Z.; Kalyanaraman, B.; Jiang, G. B. Molecular mechanism for metal-independent production of hydroxyl radicals by hydrogen peroxide and halogenated quinones. *Proc. Natl. Acad. Sci. U. S. A.* **2007**, *104* (45), 17575–17578.
- (9) Nappi, A. J.; Vass, E. Hydroxyl radical production by ascorbate and hydrogen peroxide. *Neurotoxic. Res.* **2000**, *2* (4), 343–355.
- (10) Page, S. E.; Sander, M.; Arnold, W. A.; McNeill, K. Hydroxyl radical formation upon oxidation of reduced humic acids by oxygen in the dark. *Environ. Sci. Technol.* **2012**, *46* (3), 1590–1597.
- (11) Fang, G.; Zhu, C.; Dionysiou, D. D.; Gao, J.; Zhou, D. Mechanism of hydroxyl radical generation from biochar suspensions: Implications to diethyl phthalate degradation. *Bioresour. Technol.* **2015**, *176* (0), 210–217.
- (12) Ahmad, M.; Teel, A. L.; Watts, R. J. Mechanism of persulfate activation by phenols. *Environ. Sci. Technol.* **2013**, *47* (11), 5864–5871.
- (13) Zhang, R.; Pinson, A.; Samuni, A. Both hydroxylamine and nitroxide protect cardiomyocytes from oxidative stress. *Free Radical Biol. Med.* **1998**, *24* (1), 66–75.
- (14) Waters, W. A.; Wilson, I. R. Mechanism of the oxidation of hydroxylamine by ceric sulphate. *J. Chem. Soc. A* **1966**, 534–536.
- (15) Jindal, V. K.; Agrawal, M. C.; Mushran, S. P. Mechanism of the oxidation of hydroxylamine by ferricyanide. *J. Chem. Soc. A* **1970**, 2060–2062.
- (16) Bengtsson, G.; Fronaeus, S.; Bengtsson-Kloo, L. The kinetics and mechanism of oxidation of hydroxylamine by iron(III). *J. Chem. Soc.-Dalton Trans.* **2002**, *12*, 2548–2552.
- (17) Leitner, N. K. V.; Berger, P.; Dutois, G.; Legube, B. Removal of hydroxylamine by processes generating OH radicals in aqueous solution. *J. Photochem. Photobiol., A* **1999**, *129* (3), 105–110.
- (18) Chen, L. W.; Ma, J.; Li, X. C.; Zhang, J.; Fang, J. Y.; Guan, Y. H.; Xie, P. C. Strong enhancement on Fenton oxidation by addition of hydroxylamine to accelerate the ferric and ferrous iron cycles. *Environ. Sci. Technol.* **2011**, *45* (9), 3925–3930.
- (19) Zou, J.; Ma, J.; Chen, L.; Li, X.; Guan, Y.; Xie, P.; Pan, C. Rapid acceleration of ferrous iron/oxymonosulfate oxidation of organic pollutants by promoting Fe(III)/Fe(II) cycle with hydroxylamine. *Environ. Sci. Technol.* **2013**, *47* (20), 11685–11691.
- (20) Tomat, R.; Rigo, A.; Salmaso, R. Kinetic study on the reaction between O_2 and hydroxylamine. *J. Electroanal. Chem. Interfacial Electrochem.* **1975**, *59* (3), 255–260.
- (21) Millen, M. H.; Waters, W. A. The electron spin resonance spectra of some hydroxylamine free radicals. Part IV. Radicals from alkylhydroxamic acids and amidoximes. *J. Chem. Soc. B* **1968**, No. 0, 408–411.
- (22) Bader, H.; Sturzenegger, V.; Hoigné, J. Photometric method for the determination of low concentrations of hydrogen peroxide by the peroxidase catalyzed oxidation of N,N-diethyl-p-phenylenediamine (DPD). *Water Res.* **1988**, *22* (9), 1109–1115.
- (23) Peng, S. X.; Strojnowski, M. J.; Hu, J. K.; Smith, B. J.; Eichhold, T. H.; Wehmeyer, K. R.; Pikul, S.; Almstead, N. G. Gas chromatographic-mass spectrometric analysis of hydroxylamine for monitoring the metabolic hydrolysis of metalloprotease inhibitors in rat and human liver microsomes. *J. Chromatogr., Biomed. Appl.* **1999**, *724* (1), 181–187.
- (24) Poderoso, J. J.; Carreras, M. C.; Schöpfer, F.; Lisdero, C. L.; Riobó, N. A.; Giulivi, C.; Boveris, A. D.; Boveris, A.; Cadenas, E. The reaction of nitric oxide with ubiquinol: kinetic properties and biological significance. *Free Radical Biol. Med.* **1999**, *26* (7–8), 925–935.
- (25) Finkelstein, E.; Rosen, G. M.; Rauckman, E. J. Spin trapping. Kinetics of the reaction of superoxide and hydroxyl radicals with nitrones. *J. Am. Chem. Soc.* **1980**, *102*, 4994–4999.
- (26) Zhu, B. Z.; Zhao, H. T.; Kalyanaraman, B.; Frei, B. Metal-independent production of hydroxyl radicals by halogenated quinones and hydrogen peroxide: An ESR spin trapping study. *Free Radical Biol. Med.* **2002**, *32* (5), 465–473.
- (27) Hanna, P. M.; Chamulitrat, W.; Mason, R. P. When are metal ion-dependent hydroxyl and alkoxyl radical adducts of 5,5-dimethyl-1-pyrroline N-oxide artifacts? *Arch. Biochem. Biophys.* **1992**, *296* (2), 640–644.
- (28) Anipsitakis, G. P.; Dionysiou, D. D. Radical generation by the interaction of transition metals with common oxidants. *Environ. Sci. Technol.* **2004**, *38* (13), 3705–3712.
- (29) Joo, S. H.; Feitz, A. J.; Sedlak, D. L.; Waite, T. D. Quantification of the oxidizing capacity of nanoparticulate zero-valent iron. *Environ. Sci. Technol.* **2005**, *39* (5), 1263–1268.
- (30) Andreozzi, R.; Marotta, R. Removal of benzoic acid in aqueous solution by Fe(III) homogeneous photocatalysis. *Water Res.* **2004**, *38* (5), 1225–1236.
- (31) Robinson, R. A.; Bower, V. E. The ionization constant of hydroxylamine. *J. Phys. Chem.* **1961**, *65* (7), 1279–1280.
- (32) Hughes, M. N.; Nicklin, H. G.; Shrimanker, K. Autoxidation of hydroxylamine in alkaline solutions. Part II. Kinetics. The acid dissociation constant of hydroxylamine. *J. Chem. Soc. A* **1971**, 3485–3487.
- (33) Simic, M.; Hayon, E. Intermediates produced from the one-electron oxidation and reduction of hydroxylamines. Acid-base properties of the amino, hydroxyamino, and methoxyamino radicals. *J. Am. Chem. Soc.* **1971**, *93* (23), 5982–5986.
- (34) Lind, J.; Merényi, G. Kinetic and thermodynamic properties of the aminoxyl ($\text{NH}_2\text{O}\cdot$) radical. *J. Phys. Chem. A* **2006**, *110* (1), 192–197.
- (35) Rappoport, Z.; Liebman, J. F., Eds. *The Chemistry of Hydroxylamines, Oximes, and Hydroxymic Acids*; John Wiley Press: 2009; Vol. 15, pp 611–612, 707–713.
- (36) Butler, J. H.; Gordon, L. I. Rates of nitrous oxide production in the oxidation of hydroxylamine by iron(III). *Inorg. Chem.* **1986**, *25* (25), 4573–4577.
- (37) Bengtsson, G. A kinetic study of the reaction between iron(III) and hydroxylamine in strongly acid perchlorate solutions. *Acta Chem. Scand.* **1973**, *27* (5), 1717–1724.

- (38) Johnson, M. D.; Hornstein, B. J. The kinetics and mechanism of the ferrate (VI) oxidation of hydroxylamines. *Inorg. Chem.* **2003**, *42* (21), 6923–6928.
- (39) Deng, Y. W.; Zhang, K.; Chen, H.; Wu, T. X.; Krzyaniak, M.; Wellons, A.; Bolla, D.; Douglas, K.; Zuo, Y. G. Iron-catalyzed photochemical transformation of benzoic acid in atmospheric liquids: Product identification and reaction mechanisms. *Atmos. Environ.* **2006**, *40* (20), 3665–3676.
- (40) Cooper, W. J.; Zika, R. G.; Petasne, R. G.; Plane, J. M. C. Photochemical formation of hydrogen peroxide in natural waters exposed to sunlight. *Environ. Sci. Technol.* **1988**, *22* (10), 1156–1160.
- (41) Herrmann, R. The daily changing pattern of hydrogen peroxide in New Zealand surface waters. *Environ. Toxicol. Chem.* **1996**, *15* (5), 652–662.
- (42) Tanaka, M. Occurrence of hydroxylamine in lake waters as an intermediate in bacterial reduction of nitrate. *Nature* **1953**, *171*, 1160–1161.